Journal of Building Technology, 2024, Volume 6, Issue 2
DOI: 10.32629/jbt.v6i2.2596
ISSN Online: 2717-5103
ISSN Print: 2705-1390

Seismic Vulnerability of the Prefabricated Soviet Great Panel System in Deteriorated and Transformed Buildings

Yamila C. Socarrás[1], Eduardo R. Álvarez[2]

1. Faculty of Construction, Universidad de Oriente, Avenida de Céspedes 709 altos. Esq. N. Reparto Sueño, Santiago de Cuba, Cuba.
2. Faculty of Construction, Universidad de Oriente, Calle 6 Nº16. Reparto Santa Barbara, Santiago de Cuba, Cuba.

Abstract: The prefabricated Soviet great panel system has shown good earthquake resistance performance in several countries where it has been implemented. However, there are uncertainties with the buildings built in the city of Santiago de Cuba, the area of greatest seismic danger in the country. Due to the fact that the design codes of the emergence time of the prefabricated system have already been repealed, together with the pathological damages and structural transformations carried out by the inhabitants. Therefore, a structural verification is required, through the checking of global control parameters, the eccentricities of the centers of mass with respect to the centers of stiffness, displacements and drifts of the floors, torsional stiffness, the P-Δ effects, among other aspects. Building U-142-143 is chosen for this analysis, mainly because it has critical operating conditions. It is concluded that, although the prefabricated system does not comply with all the current requirements of earthquake resistant design and present significant irregularities in plan and elevation, the building analyzed according to the formulations in the codes used, can retain rigidity in the face of seismic action. A comparison between the building according to the original project and the current variant corroborates that the greatest changes are observed in the fundamental periods. Consequently, there are variations in drift, displacement and stiffness.

Key words: structural verification; precast system; irregularities; stiffness; displacement; drifts; eccentricities

1. Introduction

Since 1964, the I-464 prefabricated system has been widely referred to as the Soviet great panel in Cuba, becoming an indispensable resource for solving housing problems. Over a period of 26 years, 665 buildings were constructed in the city of Santiago de Cuba alone, and a total of 769 buildings were built in the province of the same name. Two types of buildings (with and without balconies) were constructed, mainly consisting of 4 or 5 floors. When designing this prefabricated system, appropriate standards applicable for implementation in high seismic hazard areas were addressed, although the design specifications for the prefabricated system at the time of its emergence have been abolished. The load transfer system is cross shaped, with wet horizontal and vertical joints, and rigid at the upper structural level. The use of this system in buildings constructed in Chile and Armenia can demonstrate its good behavior during major earthquakes. There are various studies on seismic response of prefabricated reinforced concrete structures, mainly based on laboratory model tests, with a focus on nodes and connections (e.g. Clough et al., 1989; Marcus and Thiers, 2015; Kurama et al.,

2018). However, there is little research on seismic analysis of structures affected by degradation, deformation, and usage. That's why this study correctly addressed this crucial issue.

There is uncertainty in the construction of buildings in Santiago de Cuba due to pathological deterioration of structural elements and their interconnections, as well as structural modifications by residents. According to Socarras and Álvarez (2019), weight changes include water tanks and brick walls. As a result of the conversion of weight and stiffness, it is need to adjust the grid filling of the facade panel. In the case of stiffness conversion, it is need to open or remove panels and boards.

So far, research has been conducted on characterizing materials under current operating conditions and predicting seismic performance based on the oscillation period of environmental vibrations measured (T_{VA}). Socarras et al. (2020a, b) found that among the elements with pathological deterioration, the concrete quality was poor, and the compressive strength was 26% lower than that specified in the original project. Socarras et al. (2020c) evaluated the impact of some structural transformations. The conclusion drawn by Socarras et al. (2021a) is that in the three instrumented buildings, due to the deterioration of stiffness, the T_{VA} values correspond to the expected period under design seismic action. Socarras et al. (2021b) confirmed the above results through analysis.

U-142-143, located in the Jose Marti district, is one of the instrument buildings in critical operational status. Therefore, as the starting point for earthquake safety assessment, there is an urgent need to conduct structural verification on this building. Therefore, the global control parameters, current seismic design requirements, eccentricity of the center of mass relative to the center of stiffness, floor displacements and drifts, torsional stiffness, P-Δ effect, and regularity in plan and elevation are verified.

2. Materials and Methods

Two multifunctional models of the U-142-143 building were developed for dynamic analysis using ETABS V18 (CSI, 2018) based on the relationship between material properties, geometric shapes, and their constituent elements. One model reflects the building based on the original project (original variant), while the other model is the building under current conditions (current variant).

The panels are considered simply supported on a foundation and modeled like plates, as shell type finite elements that are continuously connected together to create a rigid and uniform structural system that conforms to the construction details of the joints. The stair treads are also modeled as shell finite elements connected to panels and slabs. Assuming that shell finite elements have membrane and bending properties similar to thin plates, rectangular finite elements with appropriate shape relationships are used. Figure 1 shows an isometric view of the geometric model, while Figure 2 displays the elevations of the three longitudinal and transverse axes of the original variant.

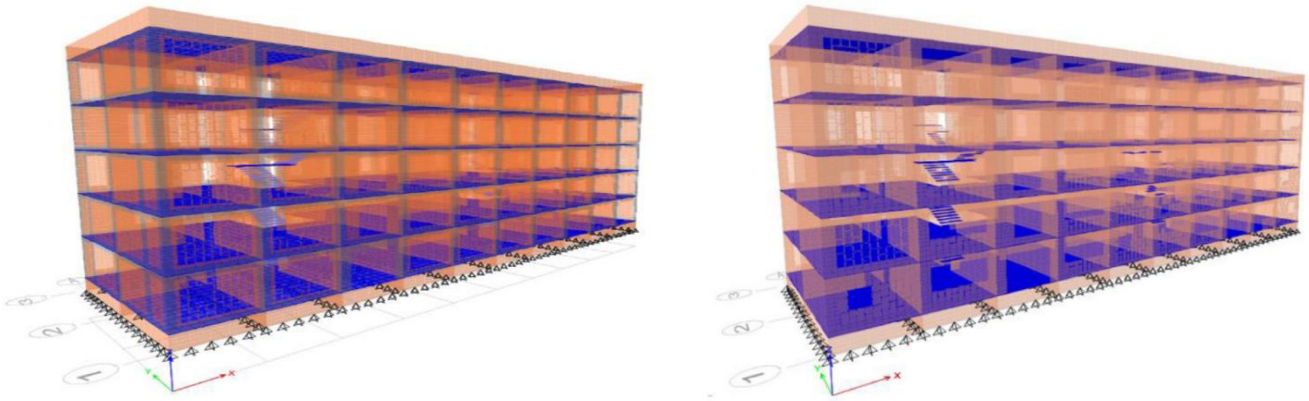

(a) (b)

Figure 1. Geometric model: (a) Original variant and (b) Current variant.

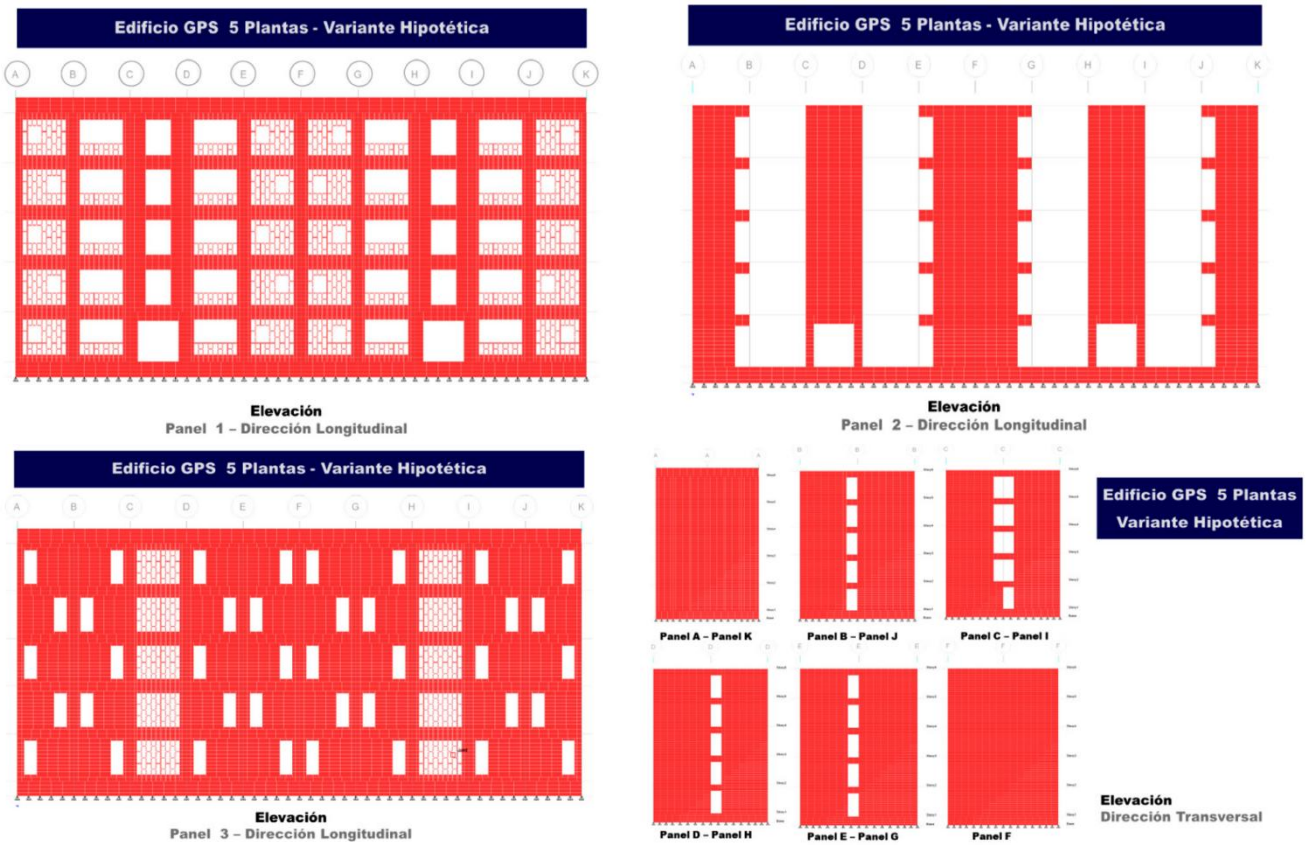

Figure 2. The elevation of the longitudinal and transverse axes. Original variant.

Building U-142-143 is a 5-story structure without balconies, measuring 32 m in length, 9.60 m in width, and 14.33 m in height. The transverse inner panels are 12 cm thick with a spacing of 3.20 m, and the longitudinal inner panels are 15 cm thick with a spacing of 4.80 m. All bi-directional outer panels are 15 cm thick in their central area, but increase to 25 cm at the edges. The thickness of the mezzanine and deck panels is 12 cm. In the current variant, the geometric shape of the pathological damage concrete section has been redefined, with a 25% reduction in thickness. The foundation is circular, with cast-in-place beams of rectangular cross-section placed on top, and small panels called pedestals placed on top. The strength of materials comes from the destructive and non-destructive tests of concrete, as well as the destructive tests of steel (Socarras, 2020; Socarras et al., 2020, 20a, b). The summary of the results is shown in Table 1.

Table 1. Material characteristics

Steel	Diameter, mm	Yield stress in elements without pathological damage f_y, MPa	Yield stress in elements with pathological damage f_y, MPa
Corrugated	9.5	328.72	205.45
	12	324.43	202.76
Non-corrugated	3	948.58	592.86
	6	397.40	248.37
	8	554.62	346.63
Concrete	Compressive strength $f'c$, MPa	Modulus of longitudinal strain E, MPa	
Prefabricated Prefabricated Backfill	16.00[a] 12.79[b] 10.00[c]	13,536.00[a] 12,102.23[b] 10,701.14[c]	

a: Prefabricated concrete in elements without pathological damage; b: Prefabricated concrete in elements with pathological damage; c: Concrete filled with trusses

The elastic modulus of precast concrete is calculated based on the expression recommended by ACI 318 (2019), but according to Lewicki's (1968) suggestion, for buildings composed of precast panels, the elastic modulus is reduced by more than 40% due to the presence of joints. On the other hand, due to the short duration of the earthquake action, the punishment increased by 20%, totaling 28%. The shear modulus G is obtained from the elastic modulus E, assuming that the Poisson's coefficient of concrete is 0.17. According to FEMA 273 (1997) and ACI 318 (2019), stiffness modifiers were used to reflect the degree of cracking and inelastic effects that occur in the elements before creep. Table 2 summarizes the bending stiffness modifiers used. In the current variant they were obtained iteratively, considering that $T_{model} \approx (1.02\text{-}1.15)T_{VA}$, as recommended by Socarrás (2020). According to Socarras et al. (2021a), the period values of T_{VA} environmental vibration were examined.

Table 2. Bending stiffness modifiers in the calibrated structural model

Element	Stiffness modifiers	
	Original variant	Current variant
Interior and exterior longitudinal panels	0.70 EI	0.35 EI
Exterior cross panels	0.70 EI	0.35 EI
Interior cross panels	0.70 EI	0.35 EI
Exterior or interior longitudinal and transverse panels with severe pathological damage	–	0.15 EI
Slabs	0.25 EI	0.25 EI
Slabs with severe pathological damage	–	0.10 EI
Filling of trusses	–	0.15 EI

The permanent load (G) and service load (Q) are defined according to the NC 283 (2003) and NC 284 (2003) standards, while respecting the considerations of the original project. As a permanent load on the deck, three layers of Alfalto coarse aggregate (0.28 kN/m^2); In the interlayer, the filling material (0.18 kN/m^2/cm), mortar (20.00 kN/m^3), and mosaic (0.23 kN/m^2/cm) are used. As a service load for the deck, drainage ditch (2.00 kN/m^2), and ordinary residential room mezzanine (1.50 kN/m^2). The self weight of the component is generated based on the specific gravity of the material (25 kN/m^3), and as it is prefabricated, it is much more compact.

In the current variant, they are added as permanent loads: water tanks in service yards, brick walls in multi-purpose areas, and grid concrete filling with some panels. According to the NC 46 (2017) standard, the response spectrum method (RSM) and equivalent static method (ESM) are used to model seismic loads using the fundamental period of modal analysis. They are considered the three basic components of earthquakes, namely horizontal and vertical, which combine 100% of seismic loads in one main direction while combining 30% of seismic loads in other directions. The vertical seismic load is modeled as an increase in the total permanent load, including the self weight of the structure. This increase is estimated to be 20% of the permanent load mentioned above, due to the short-term response acceleration specified in the design spectrum of the considered soil profile.

In each floor, unexpected eccentricity of the center of mass relative to the center of rigidity is also considered. For RSM, CQC (Complete Quadratic Combination) is used as the modal superposition formula, because it considers the proximity of modes in the response through modal correlation coefficients. As suggested by Chopra (2014), the sum of modal contribution factors is validated in units. Therefore, it must be verified that for all variants, the participation rate is at least 90%. In this work, each variant has 500 modes, and the participation rate is close to 80%. From the 500 modes, it can be seen that their contribution is negligible, so determining this value is to avoid increasing computational costs. The

design response spectrum used was drawn for residential buildings constructed in Santiago de Cuba, taking into account the location of the studied building and the reduction of the spectral y-axis assumed in the study for the energy consumption of Soviet large panels. The following provides a detailed introduction to the considerations for producing this spectrum.

A very high seismic hazard zone (5), where the maximum horizontal ground acceleration (0.30g) for the designed earthquake not only corresponds to the seismic zone, but also to the engineering category. For buildings classified as "ordinary", it is recommended to undergo a "basic earthquake" with a service life of 50 years and an acceptable exceedance probability of 10%, corresponding to a design earthquake recurrence interval of 475 years.

Soil type: Profile D, related to any thickness of rigid soil that meets the shear wave velocity standard (180 m/s ≤ vs ≤ 360 m/s), or any thickness of rigid soil profile that meets one of the following two conditions:

1) 15 ≤ N ≤ 50; N is the average number of blows in standard penetration test, blows/ft.

2) 50 kPa ≤ s_u ≤ 100 kPa; s_u is average undrained test shear strength in cohesive soil strata.

2.1 Structural system: E2 (wall system)

Ductility reduction factor R=1.5, assuming quasi-elastic response. Although NC 46 (2017) recommends a value as high as 4, it has been evaluated that they are prefabricated structures designed according to abolished standards, with poor steel ductility of structural components and insufficient details of steel reinforcement in component sections.

The load combination used is:

Combo 1: 1.2G+0.25Q+1.0Sx+0.3Sy +0.3Sz
Combo 2: 1.2G+0.25Q+0.3Sx +1.0Sy +0.3Sz
Combo 3: 1.2G+0.25Q+0.3Sx+0.3Sy +1.0Sz
Combo 4: 0.9G+1.0Sx +0.3Sy +0.3Sz
Combo 5: 0.9G+0.3Sx +1.0Sy +0.3Sz
Combo 6: 0.9G+0.3Sx +0.3Sy +1.0Sz
Combo 7: 1.2G+1.6Q

3. Results

The analysis of the structural verification of the Soviet large panel precast system is detailed below. Comparisons between the original variant and the current variant are established. Table 3 verifies the current seismic-resistant design requirements.

Table 3. Checking of current seismic-resistant design requirements in the Soviet precast large panel system

Element thickness, mm	Minimum thickness, mm	$f'c$, MPa	$f'c_{min.}$, MPa	Steel diameters, mm	f_y, MPa	f_y recommended, MPa		Bar spacing, mm		
Slab										
120	140 - 250	16.00	17.00	6	397.40	Flexure	f_{ymax} 550	150 and 200	Max.	240
				8	554.62	Shear friction	f_{ymax} 420		Min.	90
				9.5	328.72					
Panel										
120 or 150	108	16.00	17.00	3	948.58	Flexure, axial shear	f_{ymax} 550	150 and 200	Max.	360
				12	324.43					

Table 4 shows the structural response magnitudes, such as the fundamental periods of oscillation, basal shears and seismic coefficients; obtained with the ESM and RSM.

Table 4. Structural response magnitudes for building U-142-143

Original variant					
Response magnitudes			Calculation method		
			ESM	RSM	RSM (85% of ESM according to NC 46 2017)
Building weight, kN	19,005.90	Longitudinal basal shear, kN	8,742.70	6,603.0	7,431. 30
Longitudinal period, s	0.209	Transverse basal shear, kN	8,742.70	6,145.11	7,431.30
Transverse period, s	0.153	Longitudinal seismic coefficient	0.46	–	–
Torsional period, s	0.130	Transverse seismic coefficient	0.46	–	–
Current variant					
Response magnitudes			ESM	RSM	RSM (85% of the ESM according to NC 46 2017)
Building weight, kN	20,198.15	Longitudinal basal shear, kN	9,291.15	7,573.40	7,897.60
Longitudinal period, s	0.270	Transverse basal shear, kN	9,291.15	6,847.20	7,897.60
Transverse period, s	0.221	Longitudinal seismic coefficient	0.46	–	–
Torsional period, s	0.188	Transverse seismic coefficient	0.46	–	–

Table 5 and Figure 3 show the variation of the centers of mass CM and center of stiffness CR of the current variant in relation to the original variant. Likewise, Table 5 shows the eccentricities between CM and CR.

Table 5. Coordinates and changes of the mass and stiffness centers CM and CR, and eccentricities of Building U-142-143

Center of rigidity								
	Original variant		Current variant		CR Variation		CR Variation	
Floor	XCR, m	YCR, m	XCR, m	YCR, m	X, m	Y, m	X, %	Y, %
5	16.040	8.794	16.337	7.255	0.298	-1.539	1.86	-17.50
4	16.031	8.602	16.372	7.052	0.340	-1.550	2.12	-18.02
3	16.024	8.202	16.428	6.668	0.404	-1.534	2.52	-18.71
2	16.024	7.701	16.522	6.187	0.508	-1.514	3.17	-19.66
1	16.002	6.901	16.865	5.524	0.863	-1.377	5.39	-19.96
0	16.000	4.802	16.001	4.802	0.001	0.000	0.00	0.00
Center of mass								
	Original variant		Current variant		CM Variation		CM Variation	
Floor	XCM, m	YCM, m	XCM, m	YCM, m	X, m	Y, m	X, %	Y, %
5	16.003	4.815	16.000	4.800	-0.003	-0.015	-0.02	-0.31
4	15.965	4.448	15.968	4.220	0.003	-0.228	0.02	-5.13
3	15.965	4.448	15.970	4.043	0.005	-0.405	0.03	-9.11
2	15.965	4.448	15.970	4.023	0.005	-0.425	0.03	-9.55
1	15.966	4.450	16.392	4.139	0.426	-0.311	2.67	-6.99
0	15.967	4.641	16.402	4.331	0.435	-0.310	2.72	-6.68
Eccentricities in plant								
	Original variant		Current variant		Variation Eccentricity			
Floor	Ex, m	Ey, m	Ex, m	Ey, m	X, m		Y, m	
5	-0.037	-3.979	-0.337	-2.455	-0.301		1.524	
4	-0.066	-4.154	-0.404	-2.832	-0.337		1.322	
3	-0.059	-3.754	-0.457	-2.625	-0.399		1.129	
2	-0.049	-3.253	-0.552	-2.164	-0.503		1.089	
1	-0.036	-2.451	-0.473	-1.385	-0.437		1.066	
0	-0.033	-0.161	0.401	-0.471	0.434		-0.310	

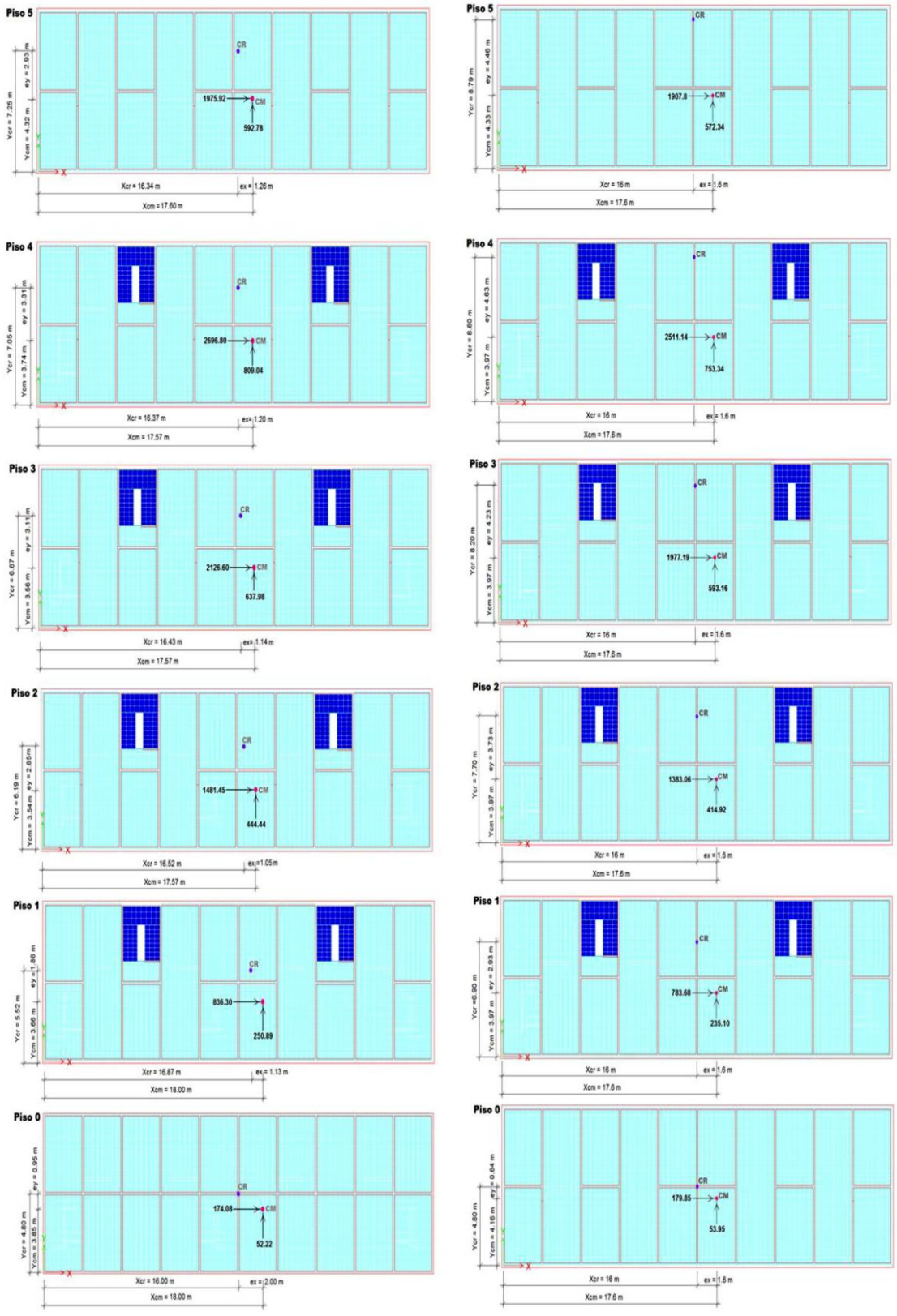

Figure 3. Positions of the centers of mass and stiffness. Current variant and original variant.

Table 6 shows the average absolute and relative horizontal displacements for the two main directions of seismic action and the relative storey rotations obtained by the ESM. Figure 4 compares the displacements between the X and Y directions of the original and the present variant.

Table 6. Displacements and drifts of the floors in the original and current variant of U-142-143

Original variant					
	Direction X			Direction Y	
Floor	Strut, m	Drift, mm	Displacement, mm	Drift, mm	Displacement, mm
5	13.50	0.824	7.157	0.791	4.629
4	10.80	1.227	6.333	0.941	3.838
3	8.10	1.543	5.106	1.022	2.897
2	5.40	1.666	3.563	0.980	1.876
1	2.70	1.624	1.898	0.768	0.896
Current Variant					
	Direction X			Direction Y	
Floor	Strut, m	Drift, mm	Displacement, mm	Drift, mm	Displacement, mm
5	13.50	1.415	12.534	1.726	10.022
4	10.80	2.210	11.119	2.057	8.297
3	8.10	2.815	8.909	2.213	6.240
2	5.40	2.961	6.094	2.115	4.028
1	2.70	2.860	3.134	1.586	1.913

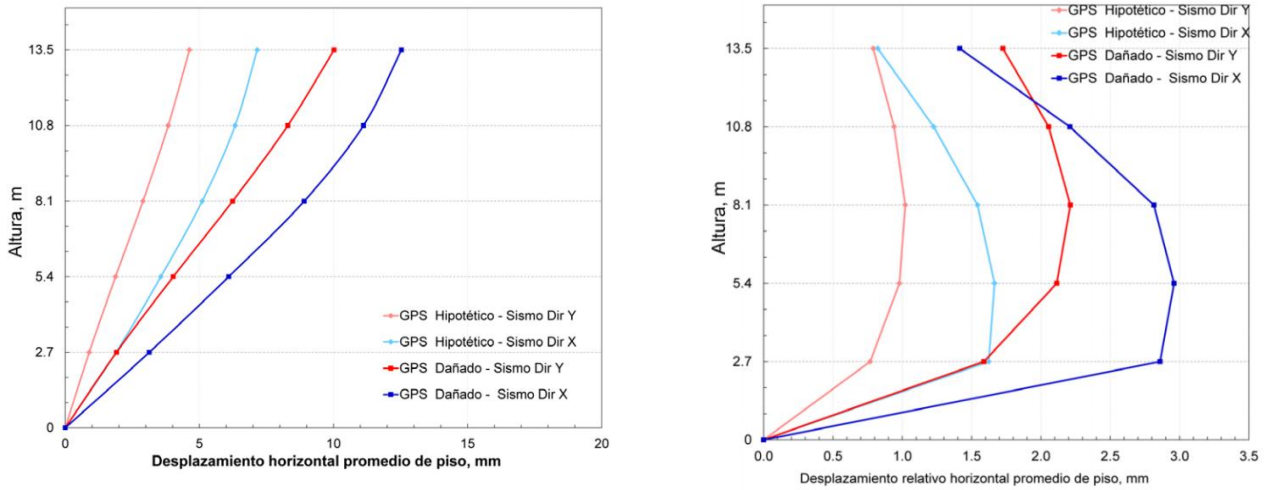

(a) Average horizontal displacement of floors, mm (b) Average horizontal relative displacement of floors, mm

Figure 4. Comparison of displacements between X and Y directions. Original Current Variant. a) Horizontal floor displacements and b) relative horizontal displacements.

Table 7 shows the torsional stiffnesses of the floors estimated with the ESM for seismic action in the X direction. Figure 5 shows the change, for each of the floors, of the relative translational and torsional stiffnesses of the current variant in relation to the original one.

Table 7. Torsional stiffness of each of the floors

Original variant			
Floor	Angular displacement, rad	Drifts angular, rad	Torsional stiffness, GNm/rad
5	0.000138	0.000026	327.19
4	0.000112	0.000030	659.24
3	0.000082	0.000031	851.00
2	0.000051	0.000029	977.23
1	0.000022	0.000021	1162.53
0	0.000001	0.000001	6554.99

Current variant			
5	0.000179	0.000032	181.25
4	0.000147	0.000040	358.23
3	0.000107	0.000043	445.02
2	0.000064	0.000038	520.73
1	0.000026	0.000024	660.58
0	0.000002	0.000002	4,718.46

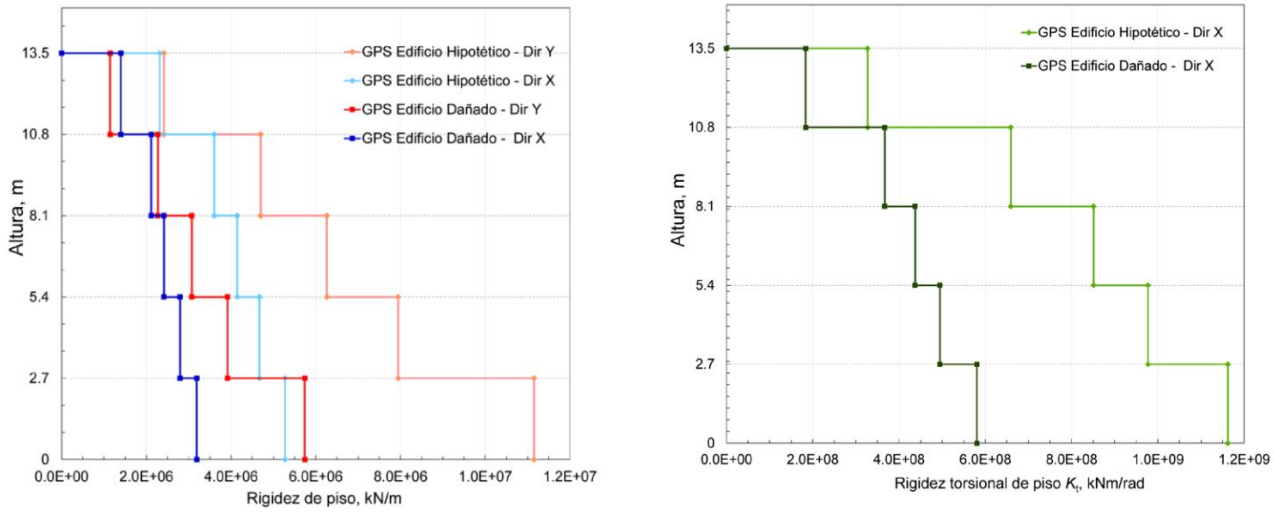

(a) (b)

Figure 5. Change in: a) floor stiffness and b) torsional stiffness

Table 8 shows the verification of regularity in plan and elevation according to NC 46 (2017).

Table 8. Verification of irregularities

Irregularity in elevation V1-A										
Original variant										
			K_i/K_{i+1}				$K_i/((K_{i+1}+K_{i+2}+K_{i+3})/3)$			
Floor	K_x, MN/m	K_y, MN/m	Dir X %	Check ≥70%.	Dir Y %	Check ≥70%.	Dir X %	Check ≥80%.	Dir Y %	Check ≥80%.
5	231.67	2,411.88	–	–	–	–	–	–	–	–
4	360.14	4,696.01	155.5	Complies	194.7	Complies	–	–	–	–
3	4,145.26	6,261.51	115.1	Complies	133.3	Complies	–	–	–	–
2	4,670.78	7,942.00	112.7	Complies	126.8	Complies	139.2	Complies	178.2	Complies
1	5,274.33	11,149.57	112.9	Complies	140.4	Complies	127.4	Complies	177.0	Complies
Current variant										
5	1,396.41	1,145.13	–	–	–	–	–	–	–	–
4	2,114.83	2,272.17	151.5	Complies	198.4	Complies	–	–	–	Complies
3	2,415.39	3,073.14	114.2	Complies	135.3	Complies	–	–	–	Complies
2	2,797.08	3,916.18	115.8	Complies	127.4	Complies	141.6	Complies	181.0	Complies
1	3,188.35	5,737.62	114.0	Complies	146.5	Complies	130.5	Complies	185.9	Complies

Irregularity in elevation V2										
Original variant										
Floor	Ws, kN	$W_{si}/W_{si-1} \leq 150\%$		$W_{si}/W_{si+1} \leq 150\%$						
		%	Check	%	Check					
5	1,300.42	69.51	Complies	–	–					
4	1,870.72	99.94	Complies	143.86	Complies					
3	1,871.92	100.00	Complies	100.06	Complies					
2	1,871.92	99.89	Complies	100.00	Complies					
1	1,873.94	95.67	Complies	100.11	Complies					
0	1,958.73	–	–	104.52	Complies					
Current variant										
5	1,300.42	64.29	Complies	–	–					
4	2,022.58	93.05	Complies	155.53	No Complies					
3	2,173.59	101.21	Complies	107.47	Complies					
2	2,147.66	101.63	Complies	98.81	Complies					
1	2,113.15	96.73	Complies	98.39	Complies					
0	2,184.51	–	–	103.38	Complies					
Irregularity in H1-A plant										
Original variant										
	(Drift max/Drift min) ≤1.5			(Drift max/Drift min) ≤1.5						
Floor	Drift variation Dir. X mm	Variation vs min value #times	Check	Variation of drift Dir. Y mm	Variation vs min value #times	Check				
5	-0.221	1.31	Complies	0.268	1.41	Complies				
4	-0.248	1.22	Complies	0.328	1.42	Complies				
3	-0.254	1.18	Complies	0.365	1.44	Complies				
2	-0.233	1.15	Complies	0.359	1.45	Complies				
1	-0.169	1.11	Complies	0.308	1.50	Complies				
Current variant										
5	-0.234	1.18	Complies	-0.431	1.29	Complies				
4	-0.273	1.13	Complies	-0.559	1.31	Complies				
3	-0.290	1.11	Complies	-0.647	1.34	Complies				
2	-0.235	1.08	Complies	-0.605	1.33	Complies				
1	-0.113	1.04	Complies	-0.340	1.24	Complies				

K_x, K_y: stiffness in relation to x or y; K_i: stiffness of level i; W_s: seismic weight; W_{si}: seismic weight of level i.

According to the NC 46 (2017) standard, Table 9 validated the P-Δ effect in the two main directions of earthquake action using ESM. In all cases, the values of coefficients C_d and β are 1.5 and 1.0, respectively.

Table 9. Verification of P-Δ effects

Original variant								
Floor	Dir - X P, kN	Dir - X V, kN	Dir - X Drifts, m	Strut, m	Dir - X Cita Adim	Value max $0.5/(\beta C_d)$ Cita Adim	Dir - X Appointment max Adim	Stability Dir - X
5	1,632.95	1,907.80	0.000791	2.70	0.00025	0.33	0.25	Complies
4	5,000.72	4,418.94	0.000941	2.70	0.00039	0.33	0.25	Complies
3	8,419.34	6,396.13	0.001022	2.70	0.00050	0.33	0.25	Complies
2	11,847.07	7,779.19	0.000980	2.70	0.00055	0.33	0.25	Complies
1	15,285.69	8,562.87	0.000768	2.70	0.00051	0.33	0.25	Complies
Floor	Dir - Y P, kN	Dir - Y V, kN	Dir - Y Drifts, m	Strut, m	Dir - Y Cita Adim	Value max $0.5/(\beta C_d)$ Cita Adim	Dir - Y Cita max Adim	Stability Dir - Y
5	1,632.95	1,907.80	0.000824	2.70	0.00026	0.33	0.25	Complies
4	5,000.72	4,418.94	0.001227	2.70	0.00051	0.33	0.25	Complies
3	8,419.34	6,396.13	0.001543	2.70	0.00075	0.33	0.25	Complies
2	11,847.07	7,779.19	0.001666	2.70	0.00094	0.33	0.25	Complies
1	15,285.69	8,562.87	0.001624	2.70	0.00107	0.33	0.25	Complies
Current Variant								
Floor	Dir - X P, kN	Dir - X V, kN	Dir - X Drifts, m	Strut, m	Dir - X Cita Adim	Valor max $0.5/(\beta C_d)$ Cita Adim	Dir - X Cita máx Adim	Stability Dir - X
5	1,632.95	1,975.92	0.001415	2.70	0.00043	0.33	0.25	Complies
4	5,162.33	4,672.72	0.002210	2.70	0.00090	0.33	0.25	Complies
3	8,905.85	6,799.32	0.002815	2.70	0.00137	0.33	0.25	Complies
2	12,626.83	8,280.77	0.002961	2.70	0.00167	0.33	0.25	Complies
1	16,318.54	9,117.07	0.002860	2.70	0.00190	0.33	0.25	Complies
Floor	Dir - Y P, kN	Dir - Y V, kN	Dir - Y Drifts, m	Strut m	Dir - Y Cita Adim	Valor max $0.5/(\beta C_d)$ Cita Adim	Dir - Y Cita max Adim	Stability Dir - Y
5	1,632.95	1,975.92	0.001726	2.70	0.00053	0.33	0.25	Complies
4	5,162.33	4,672.72	0.002057	2.70	0.00084	0.33	0.25	Complies
3	8,905.85	6,799.32	0.002213	2.70	0.00107	0.33	0.25	Complies
2	12,626.83	8,280.77	0.002115	2.70	0.00119	0.33	0.25	Complies
1	16,318.54	9,117.07	0.001589	2.70	0.00105	0.33	0.25	Complies

Cita Adim: dimensionless instability coefficient

3.1 Result analysis

The conclusion drawn from verifying the performance of prefabricated building components that meet the current seismic design requirements of ACI 318 (2019), as summarized in Table 3, is that these prefabricated components do not meet the minimum thickness required for plywood and panels, and the steel details in the panels are inappropriate because they do not have cross-sectional confinement rings to connect the two grids. FEMA 273 (1997) and FEMA 310 (1998) point out that the potential seismic damage in prefabricated panel structures is due to insufficient shear and/or flexural strength of the panels, lack of edge constraints, unsuitable longitudinal reinforcement of splice lengths, large openings, insufficient thickness, and improper connections. Therefore, the system exhibits inherent weaknesses in its design.

It also does not meet the quality of concrete, nor does it meet the steel quality of steel bars with a diameter of 3 mm, which make up the welded mesh of the panel. In addition, the creep stress of these 3 mm steel bars is higher than the

recommended value and they are smooth steel bars with non ductile behavior, as they do not have defined creep steps as observed in Socarras (2020). Carrillo and Alcocer (2013) observed sudden breakage of welded wire mesh in their experiments, suggesting that this could lead to fragile and unwelcome failure modes. For this reason, they propose that regulations should not allow a reduction in the number of steel bars in proportion to the increase in creep stress for the seismic design of walls with electric welded grids using low ductility steel as the core shear reinforcement.

Due to the use of 12 mm ductile steel in the panel, the ductility reserve of the system is limited, which to some extent depends on the stress-strain state that these steels bear due to seismic calculations. However, as demonstrated by the assumed natural ductility reduction factor of 1.5, assuming appropriate seismic performance, the system will have quasi-elastic performance.

When evaluating the global control parameters in Table 4, it can be seen that the changes compared to the original variant have the greatest increase during critical periods. By comparing the basic period of the current variant with the empirical period determined by Oliva (2001), a longitudinal period growth of 63.6% was evaluated; The lateral and torsional periods were 33.9% and 13.9%, respectively. The increase in cycle is attributed to both the decrease in rigidity caused by pathological damage and the increase in seismic weight resulting from modifications made by residents.

Compared to the horizontal period, the vertical period of these two variants is also larger. This indicates that even in the original variant, the stiffness of the structure in the longitudinal direction is relatively low. Socarras et al. (2021a) argue that considering the relationship between the length (16 m) and width (9.6 m) dimensions of buildings, they should have greater stiffness in the longitudinal direction, resulting in smaller values of the longitudinal fundamental period. However, they have greater stiffness in the transverse direction, because the area of the longitudinal panels at each level is smaller than that of the transverse panels

On the other hand, the longitudinal and transverse reference shear forces have slightly increased in the current variant, due to an increase in seismic weight rather than an increase in longitudinal and transverse periods; Because they are larger than the angular period (T1) and remain on the plateau of the spectrum. That's why the seismic coefficient of ESM remains constant in both longitudinal and transverse directions. The increment of baseline shear is 6% vertically and 15% horizontally.

From Figure 3 and Table 5, it can be seen that the building in the original variant has eccentricity on the floors and a significant eccentricity in the Y direction. This is because the windows on the rear facade (axis 3) are fewer than those on the main facade (axis 1), and even the panels on the central axis (axis 2) are weakened due to the presence of large spans to achieve multifunctional space.

In the current variant, the positions of CM and CR, as well as the resulting changes in eccentricity compared to the original variant, can be perceived. The change in CRS position is more significant than that in CM position, which is due to the weight changes of residents. In the case of grid filling, it can also lead to changes in CRS and pathological damage. Due to the increase in stiffness of the exterior wall panels caused by grid filling, in the current variant, CR deviates from axis 3 (the axis of higher stiffness), thereby reducing directional eccentricity. As a result, the seismic stress and strength of these unassembled exterior wall panels increase. However, due to the "instantaneous" nature of this rigidity, the risk of failure is further limited by the use of non-standard materials and the placement of the lattice, which are related to the pathological damage concentrated on these panels.

The results of Tables 6 and 7, as well as Figures 4 and 5, are then estimated. In both the original and the current variant, the stiffnesses in the X direction are lower (from the first to the fourth level) than in Y. Compared with the original variant, the stiffness in the X direction has decreased by 48.5%, in the Y direction by 39.5%, and in the torsion direction by

44.6%. Therefore, the displacement in the X direction is greater, 65% higher than the original variant. However, the displacement in the Y direction increased the most (113%). At the same time, the relative displacement in the Y direction is greater, only at the fifth level. Despite the increase in displacement, the drift is less than the allowable drift provided by the NC 46 (2017) standard.

Considering the use of electric welding grids for panel reinforcement, the assessment of drift may be more conservative. Carrillo and Alcocer (2013) suggested that the safety factor for the allowable drift level of walls with welded mesh should be higher than that of walls reinforced with low-carbon corrugated steel bars. Therefore, the low elongation of cold-drawn steel bars may limit their displacement capacity. This means that the allowed drift must be small, which clearly leads to a more conservative analysis.

When evaluating the displacement, it is necessary to take into account the results of Lopez and Music (2016). According to the DS61 (2011) regulation, these authors obtained displacement by considering the flexural stiffness modifier, which is lower than the displacement calculated in the order of displacement elastic spectrum, relative to the critical damping of 5%, corresponding to the cracking period of the maximum translational mass in the analysis direction multiplied by 1.3. In this study involving the review of existing building structures, the displacement obtained through the use of flexural stiffness modifiers is much more conservative than the displacement determined by approximate formulas in earthquake regulations. This leads to greater accuracy in the checking of limit states that depend on the stiffness of the system.

Considering the results in Table 8, it is reasonable to use ESM as the calibrator for the structural model. Although the studied building has significant floor eccentricity in the Y-axis direction, it has a high torsional stiffness relative to its lateral stiffness. This results in a smaller rotation of the floor relative to CR to ensure compliance with the provisions of CN 46 (2017) regarding violations H1a, V1a, and V2. Finally, from the analysis in Table 9, the P-Δ effect can be ignored as it conforms to stability validation. Although under current operating conditions, the safety margin of buildings is much lower.

4. Conclusions

The Soviet large panel prefabrication system showed inherent weaknesses in its design, as it did not meet all the requirements of current seismic design. The minimum thickness required for the slab and panel, as well as the steel details in the panel, are not suitable and do not conform to the conceptual design. It also does not meet the quality of concrete, nor does it meet the steel quality of steel bars with a diameter of 3 mm, which do not have clear creep steps. The above conditions mean that good seismic performance is only applicable to tension members that ensure the quasi-elastic performance of their structural components. The buildings analyzed under current operating conditions indicate that the fundamental periods of translational and torsional oscillations have the greatest amplification. This is due to both the decrease in stiffness caused by pathological damage and the increase in seismic weight caused by placing water tanks and adding brick walls.

Although the studied building has a significant floor eccentricity in the Y-axis direction, it has a high torsional stiffness relative to its lateral stiffness. This reduces the distortion of the floor relative to CR to a smaller value, ensuring compliance with the regulations on H1a, V1a, and V2 violations in CN 46 (2017), and proving the rationality of using ESM as a calibrator for structural models. It can also be seen that compared to the original variant, the positions of the mass center, stiffness center, and their corresponding eccentricities have changed. Specifically, by increasing the lateral displacement and distortion of the floor, the rigidity is significantly reduced. Although the lateral displacement remains within the allowable range, it complies with the specifications related to system stiffness, but the safety margin is much

smaller. Building U-142-143 can maintain stiffness under seismic action even under critical operating conditions, but it is necessary to verify the resistance of structural components and evaluate their performance, especially by changing the stiffness center position to redistribute stress and the presence of pathological damage.

The conclusion drawn from the research conducted is that special attention should be paid to the evolution of pathological injuries, as they have an impact on the structural validation of specifications that depend on system stiffness. Even under critical operating conditions, it can maintain stiffness under seismic action. Although it is necessary to assess earthquake safety, it should be done by verifying the resistance of structural elements and nodes, particularly by redistributing stress by changing the position of stiffness and mass centers, as well as by addressing existing pathological damage.

Conflicts of Interest

The author declares no conflicts of interest regarding the publication of this paper.

References

[1] ACI 318 (2019). Building code requirements for structural concrete. American Concrete Institute ACI. Washington DC, USA.

[2] Carrillo, J. and Alcocer, S.M. (2013). Shear strength of reinforced concrete walls for seismic design of low-rise housing. *ACI Structural Journal*, 110(3), 415-426.

[3] Chopra, A. (2014). Dinámica de estructuras. Pearson Educación, México.

[4] Clough, R.W., Malhas, F. and Oliva, M.G. (1989). Seismic behavior of large panel precast concrete walls: analysis and experiment. *PCI Journal*, 34(2), 42-66.

[5] CSI (2018). ETABS v18. Computers & Structures, Inc. CSI. Structural and earthquake engineering software. USA.

[6] DS61 (2011). Decreto Supremo N°61. Reglamento que fija el diseño sísmico de edificios. Ministerio de Vivienda y Urbanismo, Santiago, Chile.

[7] FEMA 310 (1998). Handbook for the seismic evaluation of buildings. Federal Emergency Management Agency FEMA. Washington DC, USA.

[8] FEMA P-154 (2015). Rapid visual screening of buildings for potential seismic hazards: A Handbook. Federal Emergency Management Agency FEMA. Washington DC, USA.

[9] FEMA 273 (1997). NEHRP guidelines for the seismic rehabilitation of buildings. Federal Emergency Management Agency FEMA, Washington DC, USA.

[10] Kurama, Y.C., Sritharan, S., Fleischman, R.B., Restrepo, J.I., Henry, R.S., Cleland, N.M., Ghosh, S.K. and Bonelli, P. (2018). Seismic-resistant precast concrete structures: state of the art. *Journal of Structural Engineering*, 144(4), p.03118001.

[11] Lewicki, B. (1968). Edificios de viviendas prefabricadas con elementos de grandes dimensiones. Arkady, Polonia.

[12] López, C. y Music, J. (2016). Análisis del período y desplazamiento de edificios de hormigón armado considerando distintos grados de rigidez en sus elementos resistentes. *Obras y Proyectos*, 19, 33-47.

[13] Marcus, J. y Thiers, R. (2015). Control del daño sísmico estructural en pórticos prefabricados de hormigón armado a través de uniones híbridas autocentrantes. *Obras y Proyectos*, 18, 46-55.

[14] NC 283 (2003). Densidad de materiales naturales, artificiales y de elementos de construcción como carga de diseño. Comité Estatal de Normalización, La Habana, Cuba.

[15] NC 284 (2003). Edificaciones. Cargas de uso. Comité Estatal de Normalización, La Habana, Cuba.

[16] NC 46 (2017). Construcciones sismo resistentes. Requisitos básicos para el diseño y construcción. Comité Estatal

de Normalización, La Habana, Cuba.

[17] Oliva, R. (2001). Determinación experimental del periodo fundamental de vibración de estructuras para la evaluación de la vulnerabilidad en Cuba. Grupo de Ingeniería Sísmica. Centro Nacional de Investigaciones Sismológicas. Cuba.

[18] Socarrás, Y.C. y Álvarez, E. (2019). Factores causantes de daños potenciales en el Gran Panel Soviético. VI Jornada Internacional de Ingeniería Civil. Holguín, Cuba.

[19] Socarrás-Cordoví, Y.C., González-Diaz, l., Alvarez-Deulofeu, E., González -Fernández, M.M., Roca-Fernández, E. and Torres-Shoembert, R. (2020a). Valuation of the durability of the concrete used in the precast Great Soviet Panel System. *Revista Facultad de Ingeniería*, 29(54), e10486.

[20] Socarrás, Y.C., González, l., Alvarez, E., González, M.M. y Roca, E. (2020b). Evaluación de la calidad del hormigón en edificaciones construidas con el sistema prefabricado gran panel soviético. *Tecnología Química*, 40(2), 264-277.

[21] Socarrás, Y.C., Alvarez, E. y Moreno, E. (2020c). Repercusiones de las contravenciones estructurales e incremento de peso en el Sistema Gran Panel Soviético en Santiago de Cuba. *Revista de Obras Públicas*, 3623, 74-82.

[22] Socarrás, Y.C. (2020). Procedimiento para la evaluación de daños sísmicos potenciales en el sistema prefabricado Gran Panel Soviético. Tesis doctoral, Universidad de Oriente, Cuba.

[23] Socarrás, Y., Álvarez, E. and Lora, F. (2021a). Forecasts on the seismic behavior of buildings constructed with the Great Soviet Panel. DYNA 88(216), 145-151.

[24] Socarrás, Y., Álvarez, E. and Lora, F. (2021b). Changes in the fundamental periods of buildings constructed with the Great Soviet Panel. *ESTOA*, 10(19), 220-235.